NIPES

Journal of Materials Engineering, Structures and Computation

Journal homepage: www.nipesjournals.org.ng

Back propagation neutral network based modelling and optimization of thermal conductivity of mild steel welds Agglutinated by Tungsten Inert Gas welding technique

Ohwoekevwo, J. U.[a], Achebo, J. I.[a], Obahiagbon, K. O.[b], Ekanem I. I.[c]*

[a] University of Benin, Department of Production Engineering, Benin City, Edo State, PMB. 1154, Nigeria,
[b] University of Benin, Department of Chemical Engineering, Benin City, Edo State, Nigeria, PMB. 1154, Nigeria,
[c] Akwa Ibom State Polytechnic, Ikot Osurua, Department of Mechanical Engineering, PMB. 1200, Nigeria,

ARTICLE INFORMATION

Article history:
Received 23 August 2023
Revised 29 August 2023
Accepted 29 August 2023
Available online 29 August 2023

Keywords:
Welding, Mild steel, Modelling, Optimization, Thermal conductivity

https://doi.org/ 10.5281/zenodo.8310192

ISSN-1115-5825/

ABSTRACT

In this study, Central Composite Design (CCD) was used to develop a Design of Experiment (DOE) for predicting thermal conductivity, allowing for the selection of weld input variables based on the ranges found in literature. The TIG welding input variables employed were the welding current, with values ranging from 199.77-250.23A, voltage ranging from 20.98-26.0 V, and gas flow rate spanning from 11.98-16.0 L/min. The design matrix deployed had six (6) centre points, six (6) lateral points, and eight (8) factorial points resulting in twenty (20) experimental runs. Thermal conductivity generated by DOE was computed using the neural network computing technique within the most suitable range. Thermal conductivity was shown to be influenced by the procedure's input variables, including welding electrical current, electrical voltage, and gas circulation rate, for both experimental and ANN simulations. The coefficient structure of the regression curve revealed R = 0.9919 for training progress, R = 0.8982 for verification outcomes, and R = 0.9979 for training validation development. This resulted in a broader Pearson correlation coefficient (R) of 0.8768, demonstrating the reliability of ANN for determining the proportion of weld dilution. The artificial neural system (ANN) model was utilized to estimate its value of proportion dilution employing identical parameters as inputs derived from the central composite design to assess the accuracy of the network it had been trained on

1. Introduction

Tungsten Inert Gas (TIG) welding also referred to as Gas Tungsten Arc Welding (GTAW) uses non-consumable electrodes to generate an arc suitable for agglutinating two or more metals together, while being shielded by inert gas such as argon or helium to protect the molten weld pool from atmospheric contaminants [1, 2]. Therefore, the tendency of atoms to bond is the fundamental basis of welding [3]. However, the selection of proper input variables to obtain the desired output response

has always been a topic of concern, not only in TIG welding applications, but in general welding techniques, as improper input variables can affect the overall weld quality. In recent times, a number of techniques have been employed in the selection of welding input variables. Some of the techniques for selecting proper welding variables is by optimization of the process parameters, using conventional numerical techniques, algorims, statistical design of experiment as well as computational networks such as Artificial Neural Network (ANN), fuzzy logic [4, 5].

Using hybrid fuzzy deep neural network, Kesse et al. [6] developed an Artificial Intelligence (AI) based TIG welding algorithm for the prediction of bead geometry for TIG welding processes. The AI TIG welding method was used to simulate a sample set that was used experimentally. Comparing the findings to the data collected during the experiment, the results demonstrated a 92.59% predicted accuracy.

Mechanical properties of Ni-base super alloy grade GH99 as employed by Korat and Sama [7] was agglutinated by GTAW technique. AI based algorithm was employed for predicting the GTAW input variables which included welding speed, current and impulse frequency as well as the output response such as tensile strength, yield strength and elongation. ANN was trained with feed-forward back propagation learning algorithm to simulate and optimize the sequence for quality weld joints. There was significant correlation between the predicted and experimental output results, which indicated that ANN can be utilized as an effective tool for computing TIG welding condition.

Saldanha et al. [8] analysed weld-bead and heat affected zones (HAZs) in TIG welding using artificial neural networks. Data used in the ANN training sequence and the feed-forward neural networks with back propagation training technique were collected via the design of experiments (DOE). Results of the ANN output response showed low error in both memorization and generalization capability, indicating that ANN is an effective tool for developing accurate models for welding process. Ohwoekevwo et al. [9] modelled and predicted the percentage dilution in AISI 1020 low carbon steel welds produced from tungsten inert gas welding using Artificial Neural Networking (ANN) approach. The regression determined exhibited R of 0.9992 as the training test outcomes, R of 0.99865 being the evaluation progress, and R of 0.85285 as the training test progress. This resulted in a total Pearson correlation coefficient (R) of 0.90007, showing that ANN is an effective approach for estimating the extent of weld dilution. There was correlation in the experimental and ANN results, as coefficient of determination (r^2 value) of 0.9876 was obtained.

The mechanical properties (Ultimate Tensile Strength (UTS), modulus of elasticity (*E*), elongation and strain (*e*) for twenty samples of AISI 4130 Low carbon steel plate were modelled and optimized by Owunna et al. [10], using ANN approach and TIG welding technique. There was proximity between the ANN predicted and experimental results which were generated for twenty (20) weld runs.

Regression analysis was carried out by Kumar and Saurav [11] based on full factorial DOE and forward-reverse modelling by controlling the five welding processes such as welding speed, wire feed rate, percentage of cleaning, work-piece to electrode gap and welding current using ANN. It was observed that the regression analysis predicted the responses accurately in some test scenarios, however, the present model could not be revised to the former. However, back propagation neural networks predicted the responses accurately and produced better results.

Regression analysis was carried out by Dutta and Pratihar [5] based on full factorial DOE and two ANN based methodologies (back-propagation algorithm and genetic-neural system). This was followed by comparing the methodologies after testing their performances on 36 test cases that were

randomly developed. For the test scenarios, it was shown that both ANN-based approaches were more adaptable than traditional regression analysis. For instance, the Genetic-neural (GA-NN) system was observed to outperform the backpropagation neural network (BPNN) in most of the test cases. Initially, slightly better performance was observed for BPNN compared to the genetic-neural system initially, but significant improvement was later recorded for the genetic-neural system after about 60,000 iterations.

Tomaz et al. [12] employed a five-factor five-level central composite design (CCD) matrix to conduct GTAW experiments. Two tubular wires were made from UTP AF Ledurit 60 and UTP AF Ledurit 68, with AISI 1020 steel blank serving as the substrate. In order to establish the ideal welding settings and simulate the GTAW process, the ANN algorithm was used in combination with a genetic algorithm (GA). Optimal welding parameters such as welding current of 222 A, welding speed of 25cm/min, nozzle deflection distance of 8 mm, travel angle of 25° and wire feed pulse frequency of 8 Hz were obtained, with R^2 of all the data higher than 0.65.

Abhulimen and Achebo [13] employed ANN in the prediction and optimization of TIG weld parameters of mild steel pipes. The Levenberg-Marquardt method and the feed-forward back propagation learning technique were used to create the neural network model. The obtained neural network model was shown to predict tensile and yield strength with a mean square error of 34.2, maximum and minimum absolute errors of 22 MPa and 0.09 MPa, according to the results. With generated average absolute variance of 15.35% and calculated average percentage error of 3.5, the largest and lowest relative errors were 18% and 0.02%, respectively.

Reference from various literature in this study revealed that several welding mechanical properties have been predicted accurately using ANN approach, but the prediction of thermal conductivity using this approach is still a gap yet to be filled, considering that very little have been done in that area. In this study, backpropagation neutral network based modelling and optimization of thermal conductivity of mild steel welds agglutinated by TIG welding technique have been employed to examine the correlations and accuracies, and possibly determine its effectiveness for application in actual case scenarios.

2. Materials and Method

Ten millimetre (10 mm) plate was obtained from Universal Steel Rolling Mill, Ogba-Ikeja, Lagos, Nigeria, and analysis for mechanical properties and chemical composition, which revealed that the material is AISI 1020 low carbon steel was determined in the same company using the mass spectrometer. The mechanical properties and composition of AISI 1018 mild steel plate are presented in Table 1.

Table 1: Properties and composition of AISI 1020 mild steel plate

Mechanical properties		**Chemical compositions**	
Melting Point	1738 K	C	0.094±0.043
Thermal expansion coefficient	1.5e-005 /Kelvin	Si	0.210±0.043
Yield strength	351.571 N/mm^2	Mn	0.310±0.73
Tensile strength	420.507 N/mm^2	P	0.056±0.40
Elastic modulus	200000 N/mm^2	Cu	0.094±0.109
Poisson's ratio	0.29	Al	0.002±0.004
Mass density	7900 g/cm^3	S	0.022±0.114
Shear modulus	77000 N/mm^2	Cr	0.214±0.073

For twenty (20) samples, the 10 mm steel plate was cut into 60x40x10 mm (long x width x width) dimensions as indicated in Figure 1. Before welding the samples, the surface of the specimen was smoothed and the rust was removed using Emery paper (coarse: P24 grit size with 715 m and fine: P80 grit size with 201 m). The surface of the samples to be welded was then cleaned with acetone to remove any surface contaminants.

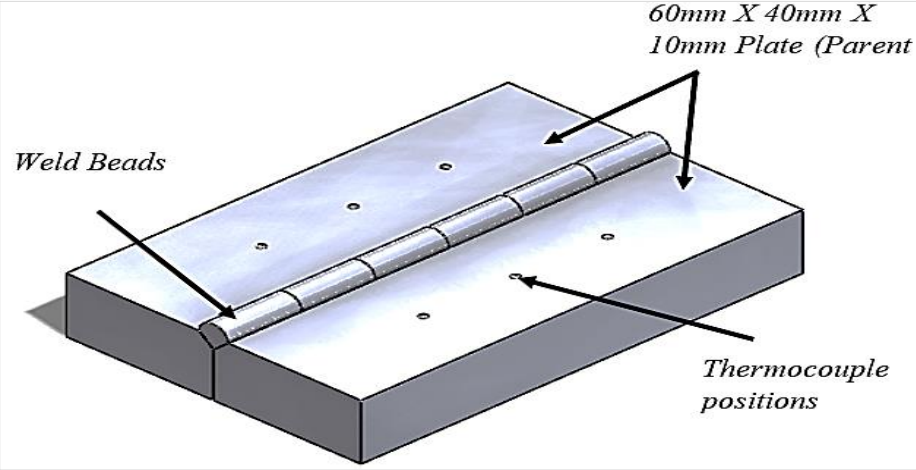

Figure 1. AISI 1020 low carbon steel plate with 10 mm thickness

The welding specimen (workpiece) was fastened to a G-clamp and chamfered (2 mm depth) with 45 degrees at the outermost point to create a V-groove angle using a vertical milling machine. A vertical milling machine was used to provide the milling angle. In order to avoid distortion during the welding process, the plates were securely secured during welding. The plate's chamfered area was TIG welded, and the chaffered area was filled with a 2% thoriated tungsten electrode. In order to safeguard the welding area from impurities, this was accomplished by using a Dynasty 210 DX welding machine and 100% Argon as the torch gas. Owunna et al.'s [14] research investigating the utilization of SEM/EDS in fractographic investigation of TIG welded AISI 1020 fusion zones at distinct welding current steps and Owunna and Ikpe's [15] study on the hardness characteristics of AISI 1020 low carbon steel weldments made by tungsten inert gas welding both used a similar methodology. Table 2 presents the TIG welding parameters used during the welding procedure, and Figure 2 displays examples of the steel plates that were welded.

Batch A Batch B

Figure 2. Mild steel welded samples

Table 2: Material specifications and welding parameters

S/N	Material Specification	Welding Parameters
i.	Welding Type	GTAW
ii.	Work piece	AISI 1020
iii.	Work piece Thickness	10 mm approx
iv.	Spec of Filler-material	ER 70 S-6
v.	Joining type	V-groove
vi.	Joining Preparation	Abrasive Clean
vii.	Gap of joint dimension	2 mm approx
viii.	Current	D.C.E.N (Direct Current Electrode Negative)
ix.	Width(wrt pulse)	0.8 Seconds
x.	Filler *Rod Angle*	15º
xi.	Torch Angle	45º
xii.	Frequency(@fixed)	60Hz fixed
xiii.	Torch spec	TIG Torch
xiv.	Tungsten spec	2% thoriated
xv.	Size of Tungsten	3/1326" (Diameter x 25.4 mm)
xvi.	Gas used	Argon
xvii.	Heat Input	10.75 KJ/min approx
xviii.	Mass of Filler Rod	78.5 Kg/m^2
xix.	Designated Machine	Dynasty 210 DX
xx.	Work piece Clamp	G-clamp
xxi.	Vertical milling Type	V-groove angle operations

The welding temperature was measured at several spots along the workpiece's surface using K-type thermocouples as the arc traveled through it. Additionally, the welding flame moved across the plate at a constant speed of 1.72 m/s while being 2.5 mm away from the workpiece. To prevent any systematic mistake in the experiment, the welding trials were conducted in accordance with the Central Composite Design Matrix (CCD) in Table 3 and in a random sequence. Design of Experiment (DOE) was employed to generate the data required by applying specific experimental limits, while also using numerical computational sequence to predict the response at any given point within the experimental boundaries.

Table 3: Central composite design matrix (CCD)

std	Weld Runs	Block	Current	Voltage	Gas flow Rate
12	1	Block 1	250.23	23.5	13.5
16	2	Block 1	225	26	14.5
10	3	Block 1	250.23	24.5	14.5
19	4	Block 1	240	25	16
6	5	Block 1	225	25	16
13	6	Block 1	240	20.98	13.5
9	7	Block 1	199.77	24.5	13.5
18	8	Block 1	210	25	16
15	9	Block 1	199.77	26	11.98
14	10	Block 1	250.23	20.98	13.5
3	11	Block 1	240	22	11.98
11	12	Block 1	225	24.5	11.98
5	13	Block 1	210	22	16
7	14	Block 1	199.77	23.5	14.5
20	15	Block 1	210	20.98	14.5
8	16	Block 1	225	22	13.5
2	17	Block 1	199.77	26	11.98
17	18	Block 1	240	20.98	13
4	19	Block 1	210	22	16
1	20	Block 1	250.23	22	11.98

According to the ASTM E1530 standard, the DTC 300 is a guarded heat flow meter that measures thermal conductivity across a wide temperature range. It used one calorimeter module for measuring thermal conductivity in the bottom stack (using three user-interchangeable stack modules) and a side guard furnace for edge heat retention. To reduce contact resistance at the sample surfaces, a pneumatic load was applied to the sample and test stack together with a thermally conductive interface material. The DTC 300 (see Figure 3) is perfectly suited for measuring thermal conductivity because of its adaptability and broadened analytical range.

Figure 3. DTC 300 equipment for measuring the weld thermal conductivity

2.1. Prediction of Thermal Conductivity Using ANN

Artificial neural networks (ANN) are computational tools designed to simulate a set data for performing specific tasks such as data classification and pattern recognition. Neural networks consist of input, output and hidden layers of units that transverses the input into ideal data that the output layer can use.

The Algorithms work well for discovering trends that are too complicated for human developers to understand and feeding them to systems for recognition. In order to get the best possible set of values, neural network models are thought of as straightforward computational models that describe a function by modifying parameters, connexion weights, or the kind of architecture, such as the number of neurons or their connections. Each artificial neuron's results is calculated through a nonlinear variation in the sum of its inputs, and each artificial neuron's signal at each point of connection between them is a real number.

'Edges' are the connections between artificial neurons. Artificial edges and neurons frequently have a weight that changes as learning advances. Artificial neurons could have a threshold that must be crossed in order for the signal to be transmitted. Signals move from the first layer, known as the input layer, to the last layer, known as the output layer, perhaps after passing through the layers more than once in order to transform the input data into the necessary set of information.

The Feedforward Multilayer Perceptron (MLP) design, in which data only flows in one way from input to output, is the ANN classifier used in this work. As seen in Figure 4, an MLP is made up of layers of processing units connected by weighted connections in a directed graph. The input variables, such as spectral bands and output classes, are comprised of the first and last layers. The internal depiction of neuronal pathways is provided by the intermediate layers, sometimes referred to as hidden layers.

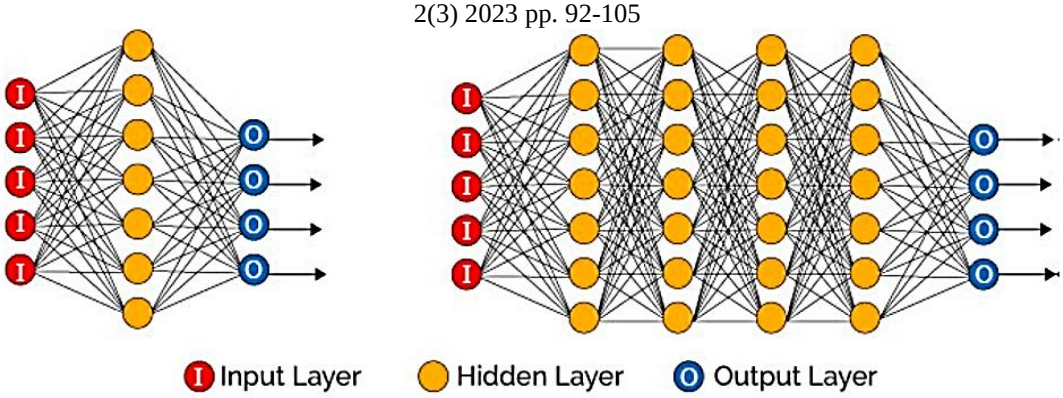

Figure 4. Profile of conventional neural network layout

The researchers who trained the network may then assign identifiers to the output and utilize backpropagation to fix any errors found both during and after the process. A built-in tool in MATLAB called the ANNs Toolbox offers functions and applications for modeling robust and complicated nonlinear situations that are difficult to represent using traditional techniques. A predictive model, such as an artificial neural network (ANN), was used in this study to predict the response variables outside the realm of experimental. Using a feed forward back propagation approach, a neural network for forecasting thermal conductivity was trained.

The output layer employs the linear (purelin) transfer function, but the input layer of the network uses the hyparbolic targent (tan-sigmoid) transfer function to compute the layer output from the network input (Owunna and Ikpe, 2019). The mean square error of regression (MSEREG) was used to track network performance, with the number of hidden neurons set at 10 per layer. An analysis update interval of 500, a learning rate of 0.01, a momentum coefficient of 0.1, a goal error of 0.01, and a maximum training cycle of 1000 epochs were all employed.

The training, validation, and testing data sets were separated from the input data during the network creation process. In this study, 60% of the data was utilized for network training, 25% for network validation, and the remaining 15% was tested for network performance. An ideal neural network design was created using these methods, and since the same input variables were used, the same network architecture was created to predict the output response variables (thermal conductivity). The network setup interphase for this study's prediction of thermal conductivity is shown in Figure 5. Figure 5 depicts the neural network establishing interphase for predicting weld variables, which served as the foundation for the neural network's design setting interphase.

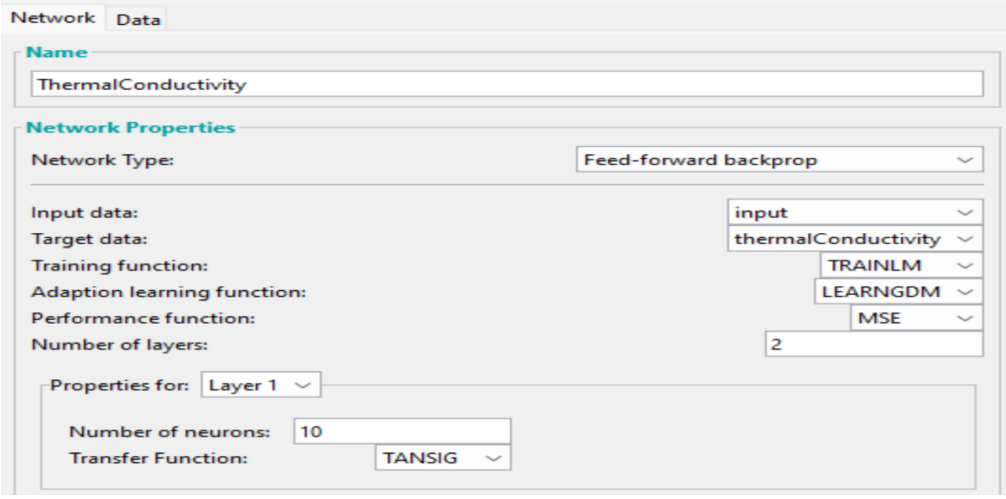

Figure 5. Network settings interphase for predicting thermal conductivity

Figure 5 shows the the default setting on ANN interphase, the feed forward backprop was chosen amongst other network type to yield the best results. Current, voltage and gas flow rate information in Table 2 were trained in ANN to predict the output response (thermal conductivity). Figure 6 presents the designed architecture for the neural network used to predict thermal conductivity. Figure 7 present the command button used for training the network. The input and targets are the factors and responses needed to predict, the output and errors are the results from the ANN trained prediction exercise.

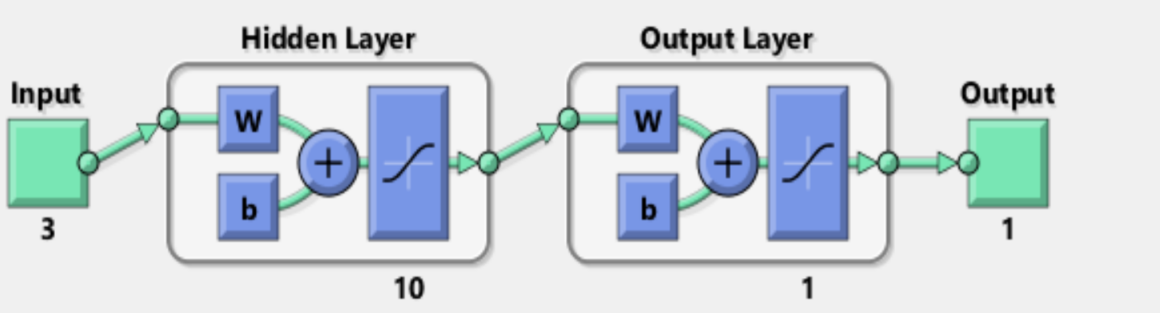

Figure 6. Artificial neural network architecture for predicting thermal conductivity

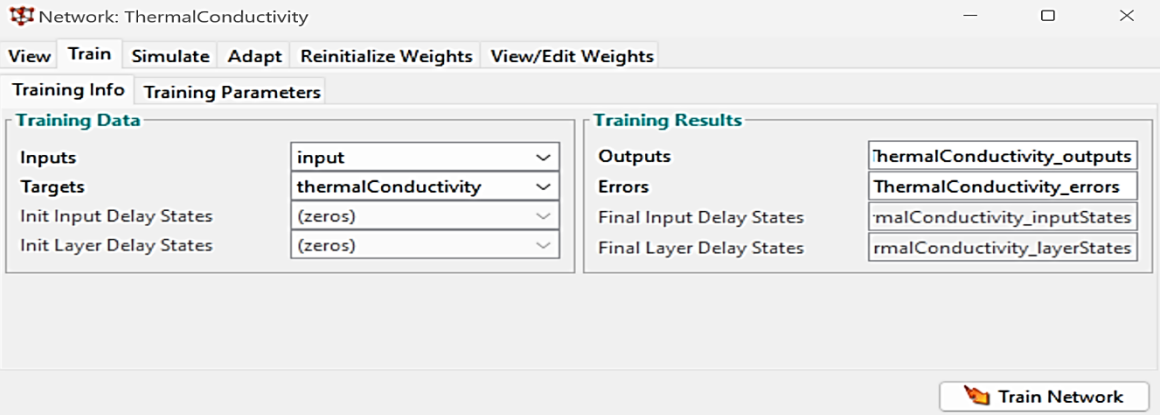

Figure 7. ANN training/retraining environment for thermal conductivity

Figure 8 present the neural network diagram for predicting the thermal conductivity. The Epoch training process undertook 13 iterations at a performance range of 1.34 with a validation check of 1.

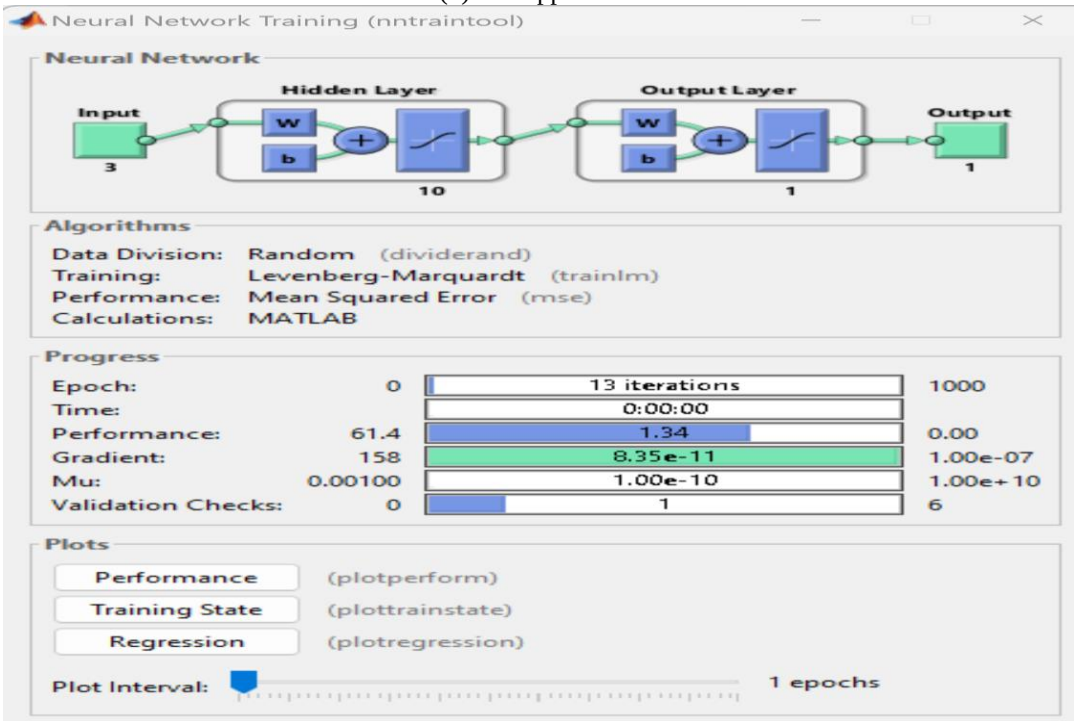

Figure 8. Network training diagram for predicting thermal conductivity

The trained network's performance curve is shown in Figure 9. At epoch 12, the highest possible validation outcome was attained. The iteration procedure employed a total of 13 epochs, with epoch 12 being the best overall with the best validation performance of 46.3052

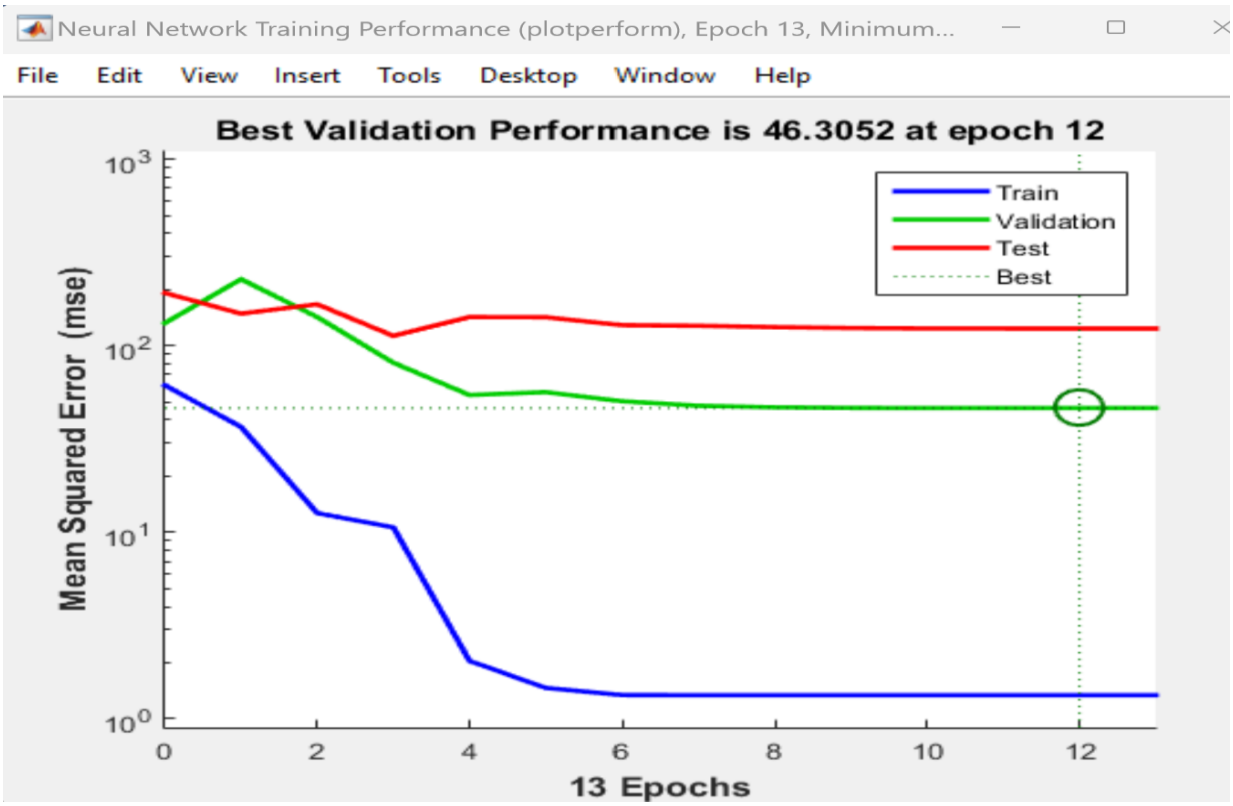

Figure 9. Performance curve for trained network to predicting thermal conductivity

3. Results and Discussion

Figure 10 displays the training state, which displays the gradient function, the training gain (Mu), and the validation check. There was no indication of excessive combining from the execution of the plot. Additionally, a similar tendency was seen in the training, validation, and testing curve behavior, which was to be expected given that the initial data set had already been normalized before usage. A key metric used to assess a network's training accuracy is lower mean square error. Figure 10 depicts the training state, which includes the slope function, training gain (Mu), and validation check for the percentage of weld thermal conductivity. It demonstrates that there were 13 training epochs. The association between the welding input parameters (welding current, voltage, and welding gas flow rate) and the expected result response (thermal conductivity) is displayed in the regression figure as seen in Figure 11.

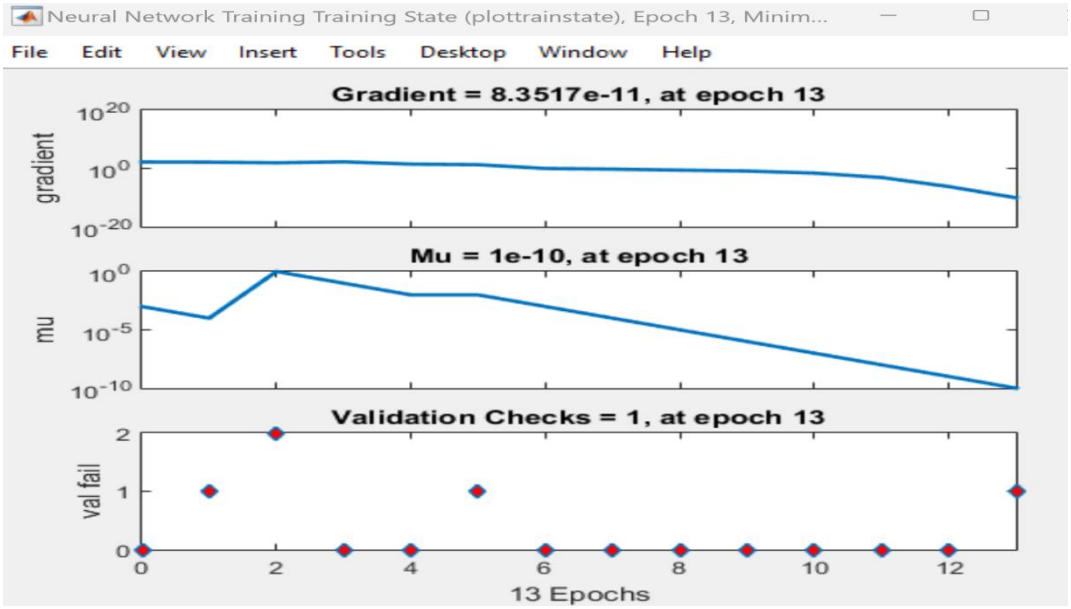

Figure 10. Neural network gradient plot for predicting thermal conductivity

Figure 11 present the training with correlation coefficient of 0.99195, validation with correlation coefficient of 0.89827 and testing with correlation coefficient of 0.99795 to give an overall correlation coefficient (R) of 0.87684 which signifies a robust prediction for the thermal conductivity. The network has been effectively trained, and may be utilized for projecting the thermal conductivity beyond the realm of testing, according to computed values of the correlation coefficient (R) as seen in Figure 11.

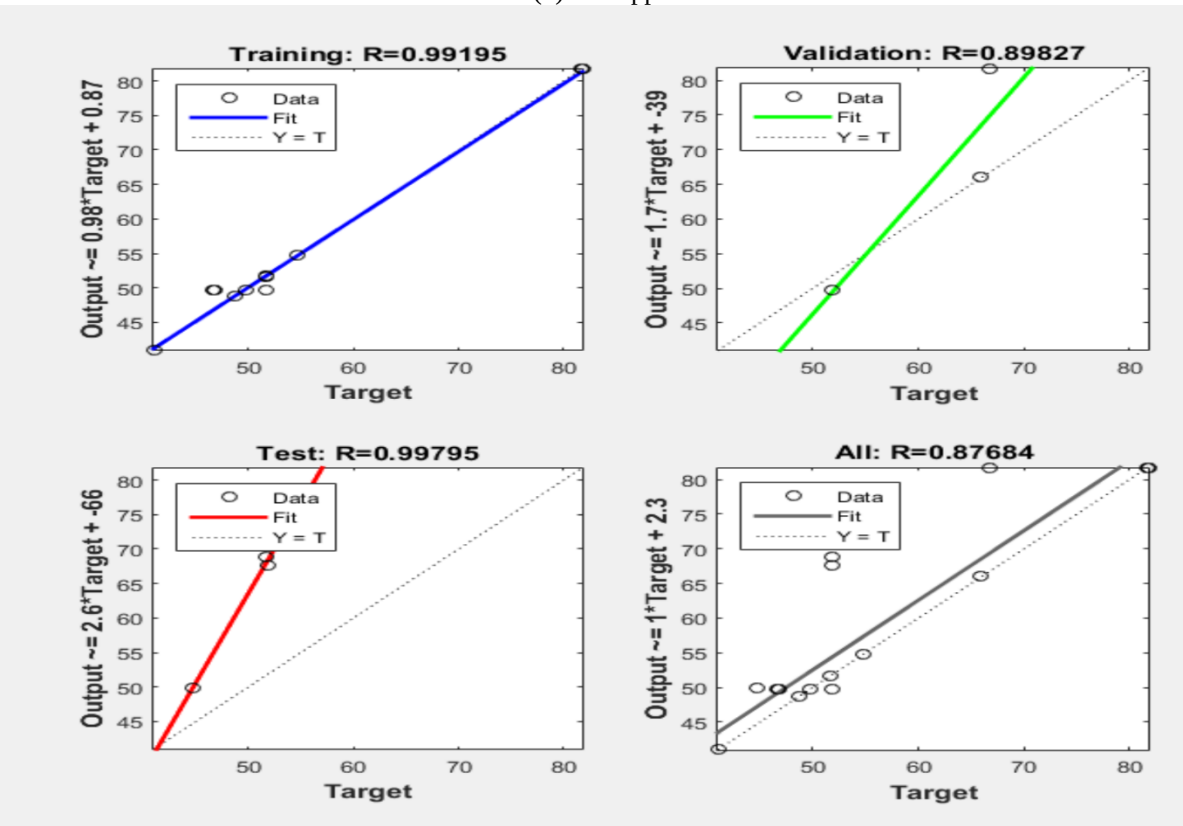

Figure 11. Plot of training (Regression plot) cum validation and testing for thermal conductivity

Using the same set of input parameters (electrical current with respect to welding operations, voltage, welding and gas flow rate) derived from the core composite design, the network was then used to anticipate its own values for percentages of weld thermal conductivity in order to assess the network's dependability. A regression plot of outputs was then created and can be shown in Figure 12 based on the observed and projected values for thermal conductivity.

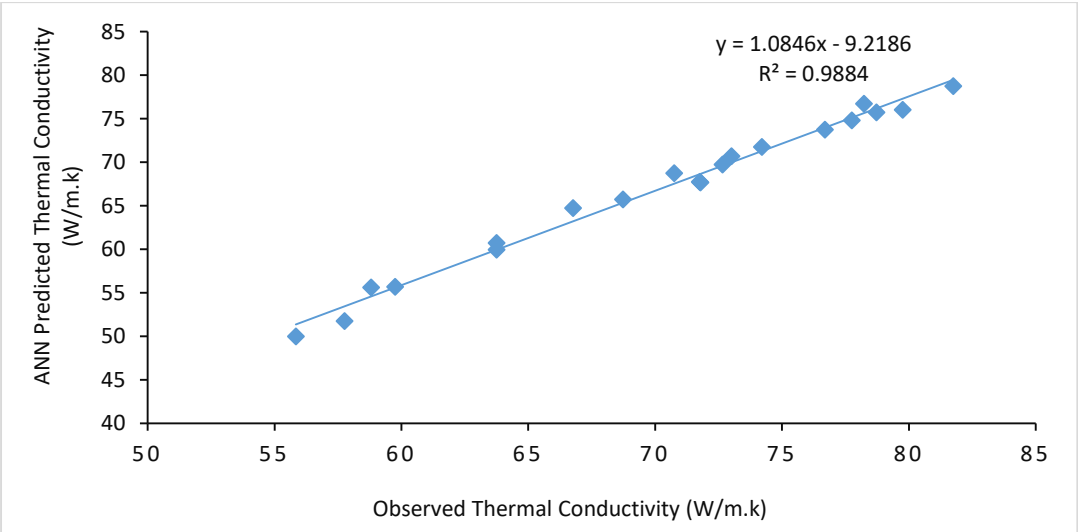

Figure 12. Plot of observed values with respect predicted thermal conductivity

Figures 12 illustrate the 0.9884 coefficient of determination (R2) value that was attained. It was concluded that the trained network can be utilized to forecast the weld thermal conductivity beyond

the experimental limit because the R2 value was near to 1. The link between the experimental and ANN projected findings for thermal conductivity is shown in Table 4.

Table 4: ANN predicted results for thermal conductivity

Weld runs	Current	Voltage	Gas flow rate	EXP thermal conductivity (W/m.k)	ANN predicted thermal conductivity (W/m.k)
1	240	20.98	13.5	70.75	68.75
2	210	22	16	68.73	65.74
3	250.23	23.5	13.5	81.75	78.74
4	210	25	16	66.76	64.74
5	250.23	20.98	13.5	79.75	76.04
6	210	20.98	14.5	63.75	60.74
7	225	24.5	11.98	74.20	71.75
8	210	22	16	72.65	69.74
9	225	26.	14.5	78.23	76.74
10	225	25	16	73.0	70.69
11	199.77	23.5	14.5	71.75	67.75
12	210	22	16	59.75	55.68
13	250.23	24.5	14.5	77.75	74.83
14	199.77	26	11.98	58.8	55.61
15	250.23	22	11.98	78.72	75.74
16	225	22	13.5	57.75	51.74
17	199.77	26	11.98	55.84	49.99
18	240	25	16	76.69	73.74
19	240	20.98	13	71.78	67.69
20	199.77	24.5	13.5	63.75	59.96

Artificial neural networks (ANNs) were used as a predictive model to forecast response variables outside the realm of investigation. For the neural network modeling, sixty (60) experimental data were produced by copying the design matrix from the CCD. Prior to normalization, the experimental data were checked for weight variation, which could lead to overexertion. The correlation between the input variables (voltage, current, and gas flow rate) and the objective variable (thermal conductivity) is depicted in the regression plot.

The network was used to forecast its own value of thermal conductivity using the same input parameters derived from the central composite design in order to assess the trained network's dependability. A regression plot of outputs was subsequently created and is shown in Figure 12 based on the recorded and projected values of thermal conductivity. R2 values of 0.9884 for the coefficient of correlation are shown in Figure 12. According to the best numerical optimization using ANN, welding material with an average thermal conductivity of 49.99 W/m.k and an R2 value of 0.9884 was generated at a current of 199.77 amps, voltage of 26 volts, and gas flow rate of 11.98 L/min.

For the same category of experimental welding inputwelding input, minimum thermal conductivity of 55.84 W/mk was obtained. Considering the optimal solution for input variables responsible for the predicted output response, this comparably indicated a difference of 5.85 W/m.k between the predicted and the experimental. The present study has succeeded in developing, predicting and optimizing welding input variables for better weld quality. Applying welding inputs such as welding current ranging from 199.77-250.23 A, voltage ranging from 20.98-26.0 V and gas flow rate ranging from 11.98-16.0 L/min, the experimental results and results obtained from AAN models developed for twenty welding runs to determine thermal conductivity was also obtained. Both experimental and ANN results graphically maintained the same trend as shown in Figure 13.

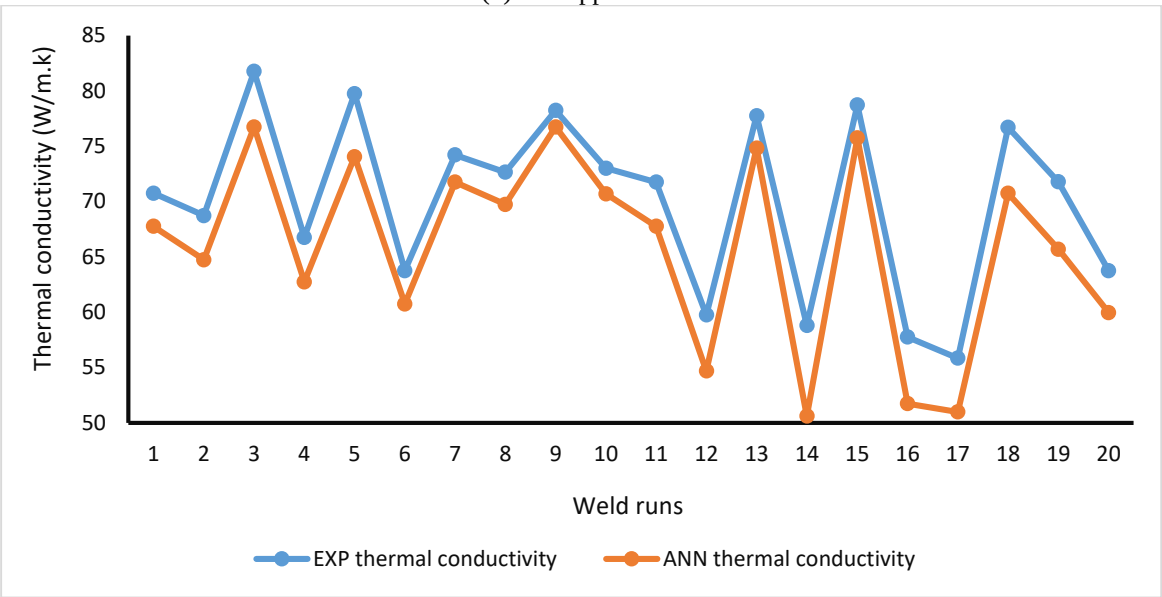

Figure 13. Series plot showing the prediction accuracy of ANN in comparison to experimental for thermal conductivity

4. Conclusion

In this study, back propagation neutral network based modelling and optimization of thermal conductivity of mild steel welds Agglutinated by Tungsten Inert Gas welding technique was successfully employed. It was observed that application of ANN was able to predict the output welding response accurately beyond the boundaries of experiment capacity, with coefficient of determination (R^2) value of 0.9884 for thermal conductivity. In practical sense, an increase in welding current will also lead to increase in thermal conductivity while voltage and gas flow rate will only produce moderate thermal conductivity. This is because the change in weld dilution and thermal conductivity of a welded joint is caused by the change in welding temperature gradient which is a function of welding current and material thermal cycle across the weldment and heat affected zone. However, this was not the exact case, as the combination of different welding input variables would interact with one another to produce weld quality that is different from the use of only one input variables. The interactions between welding parameters-the welding current with voltage can be observed to have a remarkable impact on the thermal conductivity, as high welding current and voltage input resulted in a high thermal conductivity, but can expose the material to thermally induced stress distortions at excessively high welding current and voltage. The study revealed that ANN is an effective tool that can be employed in the prediction and optimization of welding output responses particularly thermal conductivity which has been successfully demonstrated in this study.

Nomenclature

AI	Artificial Intelligence
GA-NN	Genetic-neural
GA	Genetic Algorithm
SEM	Scanning Electron Microscopy
MLP	Multilayer Perceptron
DTC	Dutch Thermoplastic Component
MSEREG	Mean Square Error of Regression
MATLAB	Matrix Laboratory
EXP	Experiment
EDS	Energy Dispersive Spectroscopy

BPNN	backpropagation neural network
ANN	Artificial Neural Network
AISI	American iron and steel institute
CCD	Central Composite Design
DOE	Design of Experiment
3D	Three dimension

References

[1] A. E. Ikpe, I. B. Owunna and E. Ikpe (2017). Effects of Arc Voltage and Welding Current on the Arc Length of Tungsten Inert Gas Welding (TIG). Int. J. Eng. Tech, Vol.3(4), pp.213-221.
[2] I. B. Owunna and A. E. Ikpe (2018). Effects of Parametric Variations on Bead Width of Gas Tungsten Arc Welding of AISI 1020 Low Carbon Steel Plate. Int. J. Eng. Tech. Sci, Vol.5(3), pp.1-13.
[3] O. D. Ikeh, A. E. Ikpe and V. Z. Njelle (2019). Effects of Electric Power Arc Inputs on the Fracture Surface and the Mechanical Properties of 0.4%C Steel. J. Sci. Tech. Res, Vol.1(3), pp.133-143.
[4] W. K. Yung, B. Ralph, W. B. Lee and R. Fenn, R. (1997). An investigation into welding parameters affecting the tensile properties of titanium welds. J. Mater. Process. Tech. Vol.63, pp.759-764.
[5] P. Dutta and D. K. Pratihar (2007). Modeling of TIG welding process using conventional regression analysis and neural network-based approaches. J. Matl Pro. Tech. Vol.184, pp.56-68.
[6] M. A. Kesse, E. Buah, H. Handroos and G. K. Ayetor (2020). Development of an Artificial Intelligence Powered TIG Welding Algorithm for the Prediction of Bead Geometry for TIG Welding Processes using Hybrid Deep Learning. Mtl, Vol.10, pp.1-14.
[7] P. Korat and M. Sama (2019). Implementation of Artificial Intelligence in TIG. Int. Conf. Adv. Comput. Mgt, `Jagannath University, Jaipur, India, April 13-14, pp.1055- 1062.
[8] S. L. Saldanha, V. Kalaichelvi and R. Karthikeyan (2018). Prediction Analysis of Weld-Bead and Heat Affected Zone in TIG welding using Artificial Neural Networks. IOP Conference Series: Matl. Sci. Eng, Vol.346, pp.1-8.
[9] J. U. Ohwoekevwo, A. Ozigagun, J. I. Achebo and K. O. Obahiagbon (2023). Prediction of Percentage Dilution in AISI 1020 Low Carbon Steel Welds Produced from Tungsten Inert Gas Welding. J. Appl. Sci. Environ. Mgt. Vol.27(4), pp.893-891.
[10] I. Owunna and A. E. Ikpe (2019). Modelling and Prediction of the Mechanical Properties of TIG Welded Joint for AISI 4130 Low Carbon Steel Plates Using Artificial Neural Network (ANN) Approach. Nig. J. Tech, Vol.38(1), pp.117-126.
[11] R. Kumar and S. K. Saurav (2015). Modelling of TIG Welding Process by Regression Analysis and Neural Network Technique. Int. J. Mech. Eng. Tech, Vol.6(10), pp.10-27.
[12] I. Tomaz, F. H. Colaço, S. Sarfraz, D. Y. Pimenov, M. K. Gupta, and G. Pintaude (2021). Investigations on Quality Characteristics in Gas Tungsten Arc Welding Process Using Artificial Neural Network Integrated with Genetic Algorithm. Int. J. Adv. Mfg. Tech, Vol.113, pp.3569-3583.
[13] I. U. Abhulimen and J. I. Achebo (2014). Application of Artificial Neural Network in Predicting the Weld Quality of a Tungsten Inert Gas Welded Mild Steel Pipe Joint. Int. J. Sci. Tech. Res, Vol.3(1), pp.277-285.
[14] I. B. Owunna, A. E. Ikpe and J. U. Ohwoekevwo (2022) Application of SEM/EDS in Fractographic Investigation of TIG Welded AISI 1020 Fusion Zones at Distinct Welding Current Steps. Arid Zone J. Eng. Tech. Env, Vol.18(2), pp.255-266.
[15] I. B. Owunna and A. E. Ikpe (2022). Hardness Characteristics of AISI 1020 Low Carbon Steel Weldment Produced by Tungsten Inert Gas Welding. Nig. J. Eng, Vol.29(1), pp.36-42.